PAPER Nr. : 60

APPLICATION OF A CONFIGURATION MODELING TECHNIQUE TO THE DESIGN AND ANALYSIS OF X-WING AIRCRAFT CONFIGURATIONS

by

D. R. Clark
Analytical Methods, Inc.
Bellevue, Washington, USA

R. T. Leitner
David W. Taylor Naval Ship Research and Development Center
Bethesda, Maryland, USA

FIFTH EUROPEAN ROTORCRAFT AND POWERED LIFT AIRCRAFT FORUM
SEPTEMBER 4 – 7TH 1979 - AMSTERDAM, THE NETHERLANDS

APPLICATION OF A CONFIGURATION MODELING TECHNIQUE TO THE DESIGN AND ANALYSIS OF X-WING AIRCRAFT CONFIGURATIONS

D. R. Clark
Analytical Methods, Inc.
Bellevue, Washington, USA

R. T. Leitner
David W. Taylor Naval Ship Research and Development Center
Bethesda, Maryland, USA

1. ABSTRACT

The correlation of an advanced configuration modeling method with wind-tunnel data for a baseline X-Wing flight demonstrator aircraft model is discussed. Modifications to the method required to handle circulation control airfoils are also described. In general, the predicted pressures are in close agreement with the experimental values on both the wing and body. Also accurately predicted are the three-dimensional separation locations. This correlated method is then used to design an unconstrained separation free hub-pylon, which is then modified to include the constraints of rotor rotation. Comparisons of pressure distributions of the baseline and new designs show significant improvement in eliminating or reducing the adverse pressure gradients at the leading and trailing edges of the hub-pylon, reducing the separation contour to a manageable thick trailing edge airfoil type. The analysis shows that a practical low drag X-Wing configuration is indeed possible.

2. INTRODUCTION

In the X-Wing aircraft, Figure 1, the benefits of a rotary wing aircraft in low speed flight and those of a more conventional, fixed-wing aircraft at higher speed are combined in a single flight vehicle. As conceived, the aircraft will be able to take off vertically, hover, and maneuver at low speed in the same way as a helicopter and, after conversion at some speed above 100 knots, fly to higher speeds as a typical aircraft with the rotor stopped and acting as a fixed wing. The design has developed as an application of the circulation control concept. Rather than by the conventional combination of mechanically induced changes of angle of attack or by varying flap or elevator settings, lift on the sustaining surfaces is modulated, both in the rotary and fixed wing modes, by the use of tangential blowing through a small slot close to the airfoil trailing edge.

The development of the circulation control airfoil concept and its application on rotary wing and fixed wing aircraft has been well documented. The feasibility of the concept is described in Reference 1 and improvements and applications of the concept conducted at the David W. Taylor Naval Ship Research and Development Center (DTNSRDC) are contained in References 2-5. A more complete list of technical publications is contained in Reference 6. Especially attractive in the rotary wing application is the potential for considerable reductions in tip speed made possible by the very high lift coefficients that circulation control airfoils offer, and the reductions in weight and complexity of the control system to be gained from the pneumatic rather than the mechanized approach. Recent work[7-8] documenting the results of full-scale rotor applications of the concept underline the potential benefits available from circulation control.

Although a very different concept from the other approaches to high speed (greater than 300 knots) rotary wing flight, such as the TRAC[9] and the ABC[10], the X-Wing has a problem in common with them. That is, the problem associated with the drag of the rotor hub assembly. As was noted in Reference 11, the drag of the hub, already large in conventional helicopters, contributes to a greater share of the total drag when the rest of the aircraft is streamlined—a necessity for high speed flight. In systems where the rotor continues to rotate, either unloaded or in a lifting only condition, some type of symmetrical rotor head fairing with its attendant sealing problems and its generally large frontal area (and hence drag) are required. On the other hand, the X-Wing, because the rotor is stopped in high speed flight, can carry an asymmetric rotor head fairing configured for minimum frontal area and minimum drag in the cruise mode. This, while not reducing the overall bulk of the fairing, does permit modeling of the hub into the overall lines of the upper fuselage with a consequent reduction in drag.

Definition of the flow field on and around even a simple rotor head fairing presents a considerable challenge, and until recently, only one option was open to a designer. That was the traditional cut and try method where the shape was modeled, tested, and modified until a converged solution was developed. Unfortunately, this process is time consuming, expensive, and, because of the unknowns associated with testing at some scale less than full size (with representative viscous effects), offers no guarantee that the end result will be repeated on the full-scale prototype. Recently, however, analytical tools have become available which permit development of a mathematical model of the configuration including the effects of viscosity and the separated flow regions. These methods, discussed in detail in References 12 through 14, allow the designer to analyze a baseline configuration and quickly and conveniently explore the effects of changes in shape. It permits him to consider many more design parameter variations and to select only the most promising candidates for model test or full-scale flight confirmation.

In this paper, the application of one such method, that of Reference 14, to the analysis and redesign of the X-Wing hub-pylon-wing root assembly will be discussed briefly, but the discussion will concentrate chiefly on the development of a practical low-drag rotor head fairing. Part of the discussion will explore how the special problems associated with modeling the rounded trailing-edge circulation control airfoils used on the X-Wing aircraft were solved.

3. THE ANALYSIS OF THE BASELINE CONFIGURATION

The analysis of the baseline aircraft, a proposed single seat 3200 pound gross weight flight demonstrator, and the subsequent redesign study were carried out using the configuration modeling program described in Reference 14. Using this code, the aircraft is modeled with a distribution of source and vorticity singularities. In a typical solution, the potential flow is calculated first. The streamline pattern is then determined and the viscous flow along the streamlines, a three-dimensional flow field, is calculated. Separation locations are determined for each streamline and the separated flow zones, if present, are defined. The effect of boundary layer and separated flow is then accounted for, not by the more conventional (but time consuming and expensive) method of changing the body shape to account for displacement thickness, but by altering the surface boundary conditions. This permits a step by step iteration to progressively include viscous effects without having to recompute the influence coefficients (the influence of each panel at every other panel) every cycle. For this study, no iterations were run.

3.1 CONVENTIONAL PANELING METHOD

The first step in the analysis is the development of a panel model of the configuration under study. Figure 2 shows the paneled baseline X-Wing configuration in a full view and in a detailed view of the hub-pylon region. Figure 3 shows the side and plan views with dimensions for reference to the location of pressure distribution and hub-pylon modifications to be described. For the calculation, the shape of the aircraft is discretized and described by a series of flat panels, each panel being represented in the solution by mathematical singularities. Source or combined source-vorticity singularities are used.

The wing on conventional aircraft, with a sharp trailing edge, is paneled with a combination of surface vorticity and source singularities. The vorticity leaves the trailing edge along a line which follows the local bisector of the trailing-edge angle, and the control point at which the vorticity strength is established lies just off the trailing edge at the midspan of the segment. On a circulation control airfoil there is no sharp "trailing edge." The separation point moves around the rounded end in proportion to the tangential momentum flux (blowing), so that the program had to be modified for the X-Wing application.

3.2 CIRCULATION CONTROL WING PANELING

Figure 4a shows cross sections of a conventional airfoil and a circulation control section as input to the program. It can be seen that without program modification, the vorticity would be shed from the airfoil at the geometric trailing edge. To overcome this, the airfoil was locally repaneled, Figure 4b, so that the effective trailing edge was moved onto the lower surface to match the known separation location. With this done, and with the vortex sheet emerging from the "new" trailing edge in a direction along the bisector of the local surface angle, the model more closely represents the real world. The airfoil modification and the repaneling to improve the flow field model was transparent to the program user, as all the repaneling had been done internally by the program from the original conventional geometric definition. The only extra information required was the local separation point. This varies, of course, with the local blowing level and the airfoil contour. Figure 5 shows a plot of potential flow calculations of the incompressible section lift coefficients versus stagnation point locations for the root and tip airfoil sections at zero degrees angle of attack. Also plotted are lift coefficients for the tip section calculated at five degrees angle of attack, corrected to zero by means of the two-dimensional lift curve slope. Similarly, lift coefficients for the root section, calculated at a higher Mach number and corrected by the Prandtl-Glauert factor are also shown. The fact that these corrections bring the points back into alignment with the zero degree curves indicates that for a given airfoil, the stagnation point location is uniquely defined by the level of blowing and is independent of both angle of attack and Mach number, at least within the range of interest.

3.3 CORRELATION OF ANALYTIC MODEL

With the completion of the baseline configuration paneling, several cases were run to provide a correlation base for the planned modification study. Data used in the correlation were taken from the test of a ¼-scale model of the X-Wing flight demonstrator shown in Figure 6, carried out in the transonic wind tunnel at DTNSRDC.* Data points which represented aircraft flight conditions of interest and for which pressure tap data were available from the ¼-scale model test were chosen for correlation. Data measurements available for the correlation cases included the total mass flow and individual total pressures at each of the blade root blowing ducts. This information, coupled with measurements of the blade slot height distribution, provided enough information to determine the spanwise blowing distribution. Given the spanwise blowing distribution, experimental tables for the blade airfoil sections were used to determine the spanwise two-dimensional lift distribution. Finally, the information in Figure 5 was used to determine the spanwise stagnation point locations shown in Figure 7. Figures 8 and 9 show examples of the correlation for these cases.

Figure 8 presents a comparison of the measured and calculated pressure distributions along the top centerline of the fuselage for a Mach number of 0.6. Pressure tap data available on the body were limited to the hub centerline and the correlation in this critical area is good. The calculations accurately predict the pressure gradients that the flow experiences as it approaches and leaves the rotor hub fairing. However, there is a slight difference between the measured and calculated data on the crown of the fairing. This has been attributed to slight differences between the shape of the model tested and that in the drawings used to develop the analytic model, to a small difference (on the order of tenths of a degree) between the actual angle of attack and that used in the calculation, and to the fact that boundary layer iterations were not run.

Figure 9 shows the spanwise variation of pressure on the upper and lower surfaces at the midchord of the forward swept wing. These data, taken for a Mach number of 0.6, show the same level of correlation.

3.4 DETAILED DESIGN ANALYSIS

A close examination of the streamline and viscous flow information generated from the calculations on the baseline configuration indicated several regions where flow separation would

*Reported informally by R. T. Leitner ("Transonic Fixed Wing Wind Tunnel Tests Of a ¼ Scale Model Of the X-Wing Flight Demonstrator," DTNSRDC/TM-16-77/133, Oct. 1977.)

occur. These are shaded on the expanded view of the hub-pylon region (Figure 10) and cross hatched where they coincided with separation zones observed on the model. As can be seen, the correlation is good. Particularly encouraging is the way in which the analysis predicted the separation zone on the upper aft portion of the hub fairing and on the aft side of the pylon just below and behind the trailing edge of the hub fairing. Also evident is a small region of separation in the stagnation zone on the hub fairing leading edge just inboard of the forward wing root.

In the latter case, the presence of separated flow on this part of the pylon is not surprising. The centerline pressure distribution plot in Figure 8 shows how the flow is accelerated over the top of the cockpit canopy and is then very severely decelerated as it approaches the leading edge of the pylon. In addition, the flow here divides to pass above and below the fairing, and at the same time meets the flow coming in along the leading edge of the forward wing.

The flow over the aft portion of the hub fairing is more complex. Over the upper surface the strong aft-facing curvature dominates, causing a severe unfavorable pressure gradient that precipitates separation. On the lower surface of the fairing and on the sides of the pylon similar unfavorable gradients prevail. The whole picture is complicated by the effects of the wing lift carryover onto the fairing. This is particularly evident on the aft face of the fairing where the natural effect of the change in shape and the carryover onto the hub of the unfavorable gradients along the trailing edge of the aft wing combine. Figure 11 illustrates this. Here, the pressure distributions along cuts parallel to the centerline are superimposed. In all the plots, the upward pointing triangles are for upward facing surfaces and the downward pointing triangles for downward facing surfaces.

Starting from the most outboard section at buttline 24.0, the cut passes through both wings and the aft loaded characteristic of the circulation control airfoils is seen. Of particular note, in terms of its impact on the flow over the airframe, is the strong unfavorable pressure gradient on the lower surface of the aft wing. The next section, at buttline 16.0, is taken where the wings and the hub fairing have begun to merge. The forward wing leading edge and aft wing trailing edge pressure peaks are still preserved, but between them the averaging effect of the presence of the fairing can be seen. At buttline 13.0 the merging continues and at 10.0 the cut involves only the pylon. Despite this, the effect of the wing lower surface leading edge suction peak persists, and the unfavorable gradient on the lower surface trailing edge is still present. The final cut is along the centerline, buttline zero.

Aggravating the problems on the hub lower surface and especially on the aft side of the pylon is the shape of the "channel" through which the air flows. This is illustrated by the sections through the hub-pylon assembly shown in Figure 12. These sections in the region where hub fairing and pylon merge show converging surfaces meeting in a cusplike form. Even under ideal conditions, when the flow is uniform, boundary layer growth in these cusplike regions is accelerated; when unfavorable gradients are present, the effects are magnified.

In reviewing the problems on the baseline hub fairing and pylon, they all appear to spring from the attempt to use a "conventional" ellipsoidal rotor head fairing. This is responsible for the large frontal area, for the extreme pressure gradients on the approaches to the pylon (the stagnation against the front and the rapid expansion over the brow of the hub fairing immediately after the strong expansion over the crown of the canopy), and for the overly rapid recovery in the lee of the hub fairing. It also produces the cusplike channel on the region bounded by the hub fairing lower surface, the pylon side, and the curve of the upper fuselage with the resulting aggravated boundary layer growth and eventual separation on the pylon side. To avoid these problems, a change must be made from the conventional approach of a fairing configured to satisfy rotational symmetry requirements to one which more closely follows the overall lines of the high-speed aircraft. It was this idea that directed the redesign of the pylon as it will be described in the next section.

4. DEVELOPMENT OF THE MODIFIED HUB FAIRING AND PYLON

4.1 *FAIRING DESIGN UNCONSTRAINED BY ROTATION*

In an attempt to avoid the problems associated with the ellipsoidal fairing noted above, a new design was developed. This is presented in Figure 13, and for comparison, the outline of the earlier fairing is superimposed. Other changes incorporated in the new design are a reduction in forward shaft tilt from four degrees to one degree, and the elimination of blade precone. The first modification was arrived at without applying any constraints relative to practicality from the point of view of having to rotate in the helicopter mode and was designed to give minimum drag in the forward flight, wing fixed condition.

The fairing shape was developed between two basic defining sections. They were the minimum profile required on the centerline to enclose the pneumatic valving system and blend smoothly into the crown of the cockpit and the aft pylon, and a section at aircraft buttline 20.0 to enclose the envelope of maximum excursion of the blade root airfoils and provide a streamlined fairing around the root mechanism. The forward portion of the centerline section was designed to blend smoothly with the crown of the canopy, avoiding the sudden changes in profile that resulted in the large excursions in surface pressure on the baseline. The aft portion was configured to provide as gentle a recovery as possible from the suction peak on the crown of the fairing. The buttline 20.0 section was conceived as airfoil-shaped, maintaining as long a run of constant pressure on the upper and lower surfaces as possible, delaying recovery until as close to the trailing edge as was practical. A small amount of aft camber was added to help match conditions in the region where flows from the upper surface and those on the lower surface and along the pylon sides recombine at the trailing edge. The leading edge was also cambered (drooped) to put the mean line as much as possible along the direction of the onset flow, which in this region is deflected upwards under the influence of the fuselage.

Between these two sections, the surface was blended to provide a smooth fairing over the machinery and the nonrotating hub assembly. The hub-pylon region was filled out to avoid the cusp-like region noted on the baseline. This filling is especially noticeable on the front view comparison of Figure 13. Several variations of the shape were run through the program, examining pressure distributions and boundary layer growth until a final shape was developed. This retained the basic defining sections of the first try and was different only in the details of the transverse fairing.

The pressure distributions of the redefined fairing and the baseline ellipsoidal are compared in Figure 14. Most noticeable is the relief of the strong changes in the pressure distribution ahead of the fairing and the dramatic reduction in the unfavorable gradient on the aft pylon. No boundary layer separation was calculated for the new fairing, whereas on the ellipsoidal, extensive separation was noted at fuselage station 180.0. Boundary layer growth along the sides of the new pylon was similarly well behaved. Because of the more slender, airfoil-like shape, the flow over the hub fairing was predominantly two-dimensional and substantial amounts of lift were generated, particularly on the aft portions. This resulted in a considerable downward deflection of the stream as it leaves the hub. If any separated flow were present, this would be carried down and below the horizontal stabilizer and any antitorque device.

4.2 FAIRING DESIGN CONSTRAINED BY ROTATION

Having developed a separation free (long) aerodynamic fairing, the analysis was then used to explore ways in which the fairing could be shortened in order to arrive at a more practical, rotatable shape. This was developed by simply cropping the fairing shape behind the aft wing until a shape was produced which had the minimum practical airfoil-like trailing edge. The criterion in the shortening process was that separation should not occur more than 5 percent of the fairing chord ahead of the trailing edge. The resulting (short) fairing is shown compared with the long fairing in Figure 15.

The forward shape has been maintained and all the changes restricted to the aft end. The amount of trailing-edge camber has been increased and with the increased trailing edge angle this steepens the pressure gradient, Figure 16. But as can be seen, attached flow has been maintained until very close to the trailing edge. A manageable separated flow is generated, much like that on a thick trailing-edge airfoil. A fairly thin region of separated flow is produced which will be convected downwards under the influence of the strong aft loading. Another noticeable feature, contributing to the steepening of the unfavorable pressure gradient on the aft portion of the short fairing is the coalescence of the suction peaks of the aft camber and the carryover from the aft wing. On the long pylon, these are separate and distinct, whereas on the short pylon, because of the cropping, they combine.

In Figure 17, the centerline pressure distributions on the three hub fairings are compared. Here, the dramatic changes in the forward and aft pylon pressure gradients as the shape was progressively modified are clear. It also puts into perspective the increase in unfavorable aft pressure gradient between the long (separation free) and short (more practical) modified fairings. Although producing a much stronger effect than the ideal shape, the short fairing is still considerably better than the baseline ellipsoidal triggering only a small but manageable separated flow. On the ellipsoid, the continued curvature over the top of the fairing tended to submerge the carryover effect from the wings. On the modified fairings, with long relatively flat upper surfaces, the carryover is more pronounced, but the run of unfavorable pressure gradient in the region between the wings is short and did not have a serious impact on boundary layer conditions. The boundary layer growth along the centerline of all three fairings at a similar flight condition is summarized in Figure 18.

On both the long and short fairings, the edge at buttline 20.0 was simply cut off, providing a flat surface onto which the wings were butted. On the aircraft, this should introduce no aerodynamic problems since the calculated flow is strongly two-dimensional except in the immediate vicinity of the forward wing leading edge and aft wing trailing edge. If an edge separation did occur, it would produce a tightly rolled up local vortex which would develop streamwise, effectively fairing the edge. The edge could also be faired with a simple revolved fairing and exploration of this detail is planned.

5. CONCLUSIONS AND RECOMMENDATIONS

In the work described in this paper, a mathematical model of the configuration has been used to analyze a baseline configuration of the X-Wing aircraft and to develop modifications to the hub-pylon region aimed at reducing drag and separated wake flow. While a final conclusion on the accuracy of the analysis and a judgement on the success of the redesign effort must await further wind-tunnel verification, the redesign exercise has shown that numerical analysis of the type used can play a powerful role in the design process. The combination of the ability to generate the potential flow field and then the resulting viscous flow behavior allows a reasonably rapid estimate to be made of the effect of changes in shape. The combination also permits a wide range of possible configurations to be easily and inexpensively investigated before concentrating on the most promising for detailed study and testing.

As with any investigation of this type, several factors emerged that would merit further study. Most promising, from the point of view of reducing drag, would be an examination of the effect of reducing the loading of the inboard portions of the wing on the carryover, and hence the unfavorable pressure gradients on the aft pylon. This can be calculated very easily, but would require a considerable investment of test time to explore. Another area which should be studied is the behavior of the fairing shapes at some orientation to the onset flow other than the final parked position. An estimate could be made of the fluctuations in lift, moment, and drag in the last stages of slow down by calculating the flow around the configuration with rotor and fairing at a number of azimuthal settings. The associated separated wake influence on the empennage could also be analyzed. This work is continuing.

6. ACKNOWLEDGMENTS

The authors wish to acknowledge the contributions of their colleagues at Analytical Methods and at DTNSRDC. Support for this research was provided by the Lockheed California Company and the Defense Advanced Research Projects Agency.

7. REFERENCES

1) I. C. Cheeseman and A. R. Seed, The Application of Circulation Control by Blowing to Helicopter Rotors, Journal of the Royal Aeronautical Society, Vol. 71, No. 848, Jul 1966.

2) R. M. Williams and H. J. Howe, Two-Dimensional Subsonic Wind Tunnel Tests on a 20-Percent Thick, 5-Percent Cambered Circulation Control Airfoil, NSRDC Report ASED-176 (AD 877-764), Aug 1970.

3) R. J. Englar, Two-Dimensional Subsonic Wind Tunnel Tests of Two 15-Percent Thick Circulation Control Airfoils, NSRDC Report ASED-211, Aug 1971.

4) J. B. Wilkerson, et al., The Application of Circulation Control Aerodynamics to a Helicopter Rotor Model, Jol. of the American Helicopter Society, Vol. 19, No. 2, Apr 1974.

5) R. M. Williams, Application of Circulation Control Rotor Technology to A Stopped Rotor Aircraft Design, First European Rotorcraft and Powered Lift Aircraft Forum at Southampton, England, 22-24 Sep 1975.

6) R. J. Englar, et al., Circulation Control — An Updated Bibliography of DTNSRDC Research and Selected Outside References, DTNSRDC Report 77-0076, Sep 1977.

7) Design Study of a Flight Worthy Circulation Control Rotor System, Kaman Aerospace Corporation Report R-1036-2, Contract N00019-73-C-0429, Jul 1974.

8) Final Report X-Wing Vehicle Design Study and Composite Blade Design, Lockheed Report SP-4601, Contract N00600-76-C-1506, Jun 1977.

9) E. A. Fradenburgh and N. F. K. Kefford, Cost-effectiveness Benefits of a Variable Diameter Rotor System As Applied to Advanced VTOL Aircraft, Presented at the American Helicopter Society Symposium on Rotor Technology, Aug 1976.

10) A. J. Ruddell, Advancing Blade Concept (ABC™) Development, 32nd Annual National V/STOL Forum of the American Helicopter Society, Wash., D.C., Paper 1012, May 1976.

11) D. R. Clark and T. W. Sheehy, A Method for Predicting Helicopter Hub Drag, USAAMRDL-TR-75-48, Jan 1976.

12) F. A. Woodward, et al., A Computer Program for Three-Dimensional Lifting Bodies in Subsonic Inviscid Flow, USAAMRDL-TR-74-18, Apr 1974.

13) F. A. Dvorak, et al., Investigation of Three-Dimensional Flow Separation on Fuselage Configurations, USAAMRDL-TR-77-4, Mar 1977.

14) D. R. Clark, et al., Helicopter Flow Field Analysis, USARTL-TR-79-4, Apr 1979.

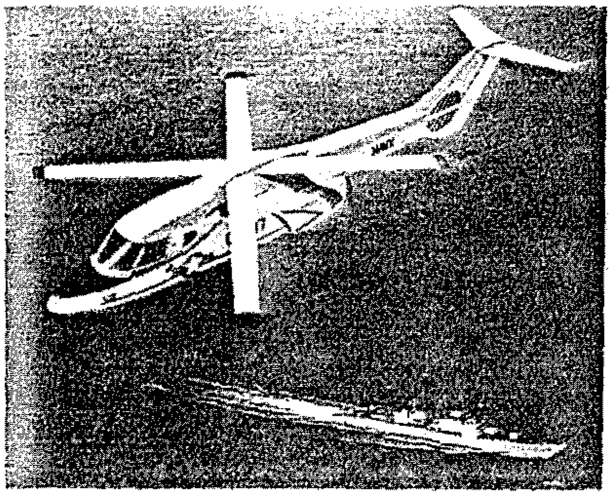

Figure 1 — X-Wing Aircraft Concept

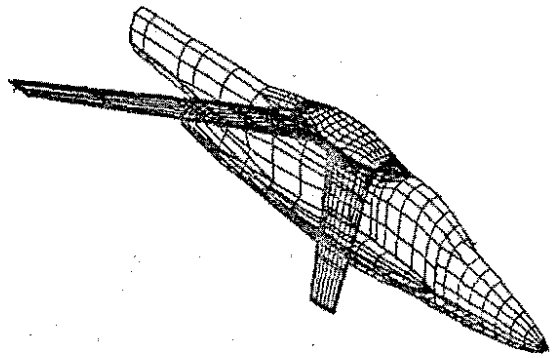

Figure 2a — Complete Model

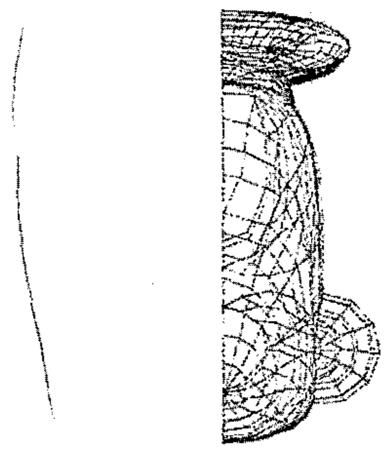

Figure 2b — Rotor Head Fairing Detail

Figure 2 — Baseline Paneled Model

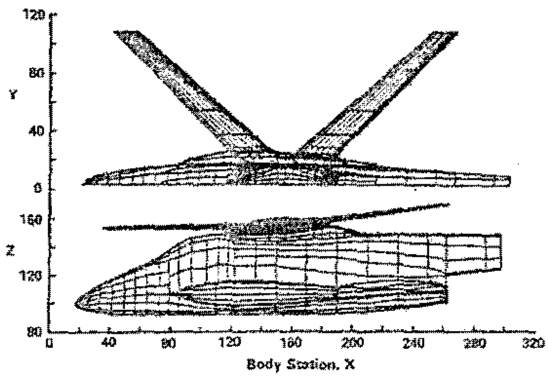

Figure 3 — Baseline Paneled Model Coordinates

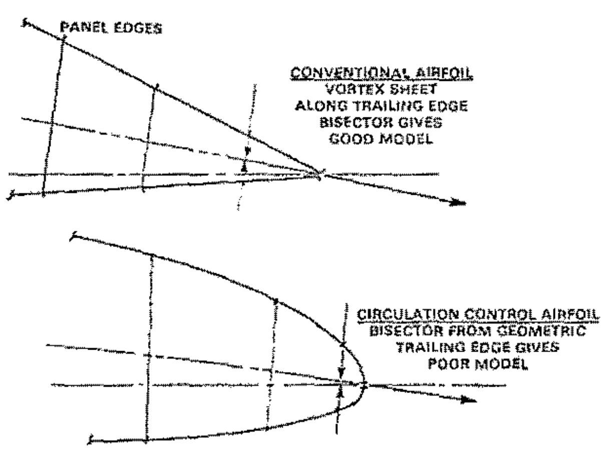

Figure 4a — Conventional Airfoil Paneling Method

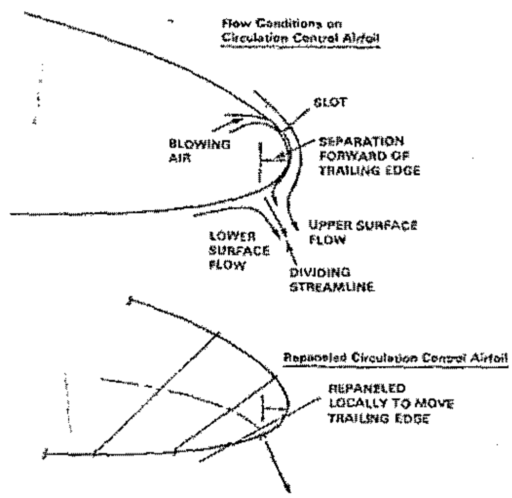

Figure 4b — Modeling of Stagnation Point Movement with Blowing

Figure 4 — Wing Paneling Methods

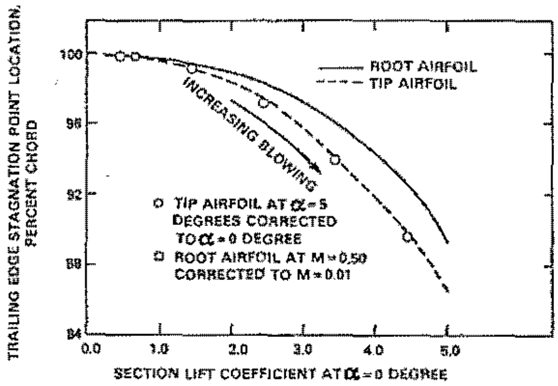

Figure 5 — Two-Dimensional Variation of Stagnation Point with Blowing

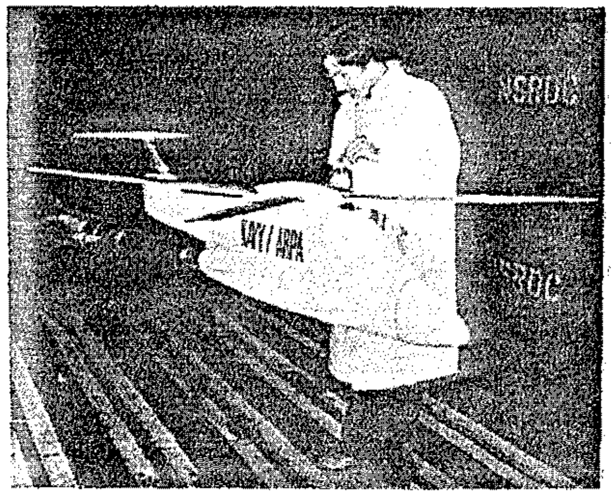

Figure 6 — Transonic Model (¼ Scale) of Baseline Flight Demonstrator

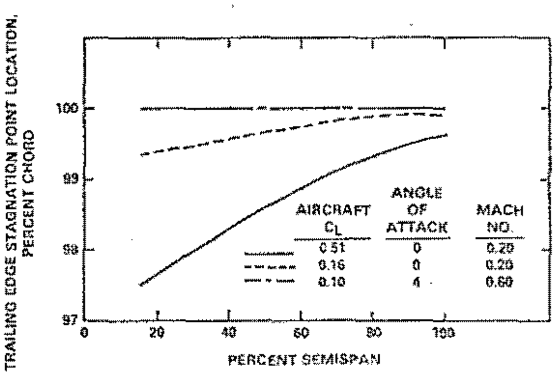

Figure 7 — Spanwise Stagnation Point Location for Baseline Correlation Cases

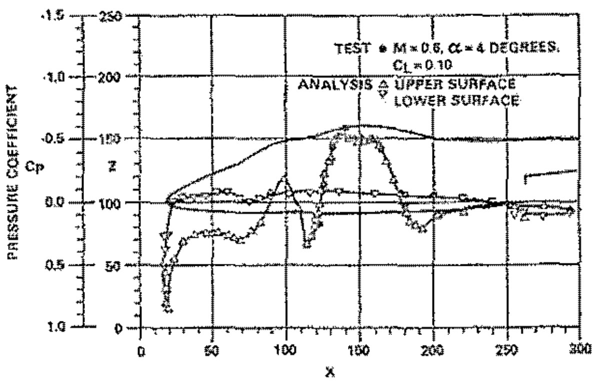

Figure 8 — Baseline Hub Centerline Pressure Distribution

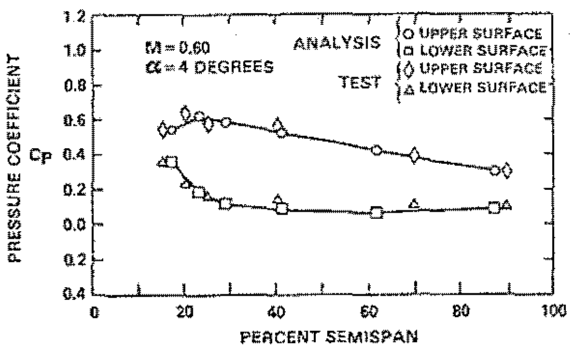

Figure 9 — Baseline Forward Wing Midchord Pressure Distribution

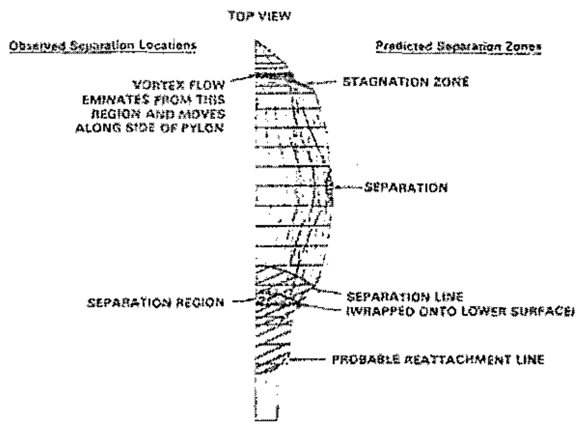

Figure 10 — Predicted and Observed Separation Locations on Baseline

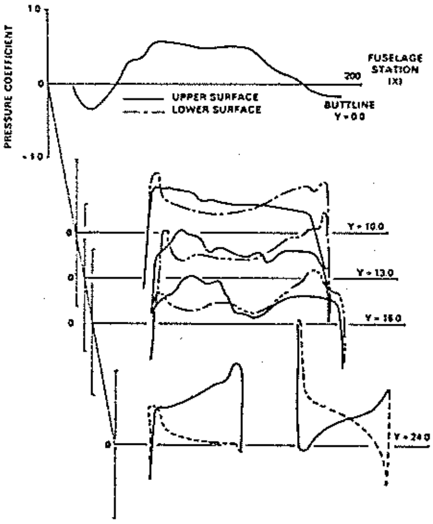

Figure 11 — Effect of Wing Lift on Hub Fairing Pressures

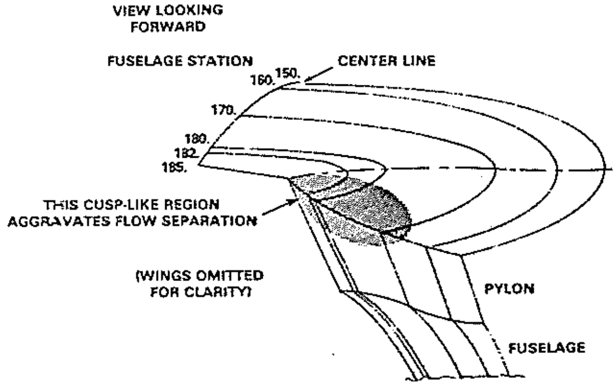

Figure 12 — Vertical Cuts through Baseline Aft Hub-Pylon

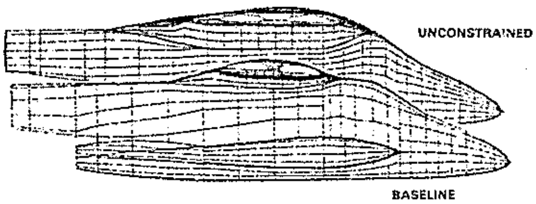

Figure 13 — Comparison of Baseline and Rotation Unconstrained Fairing Designs

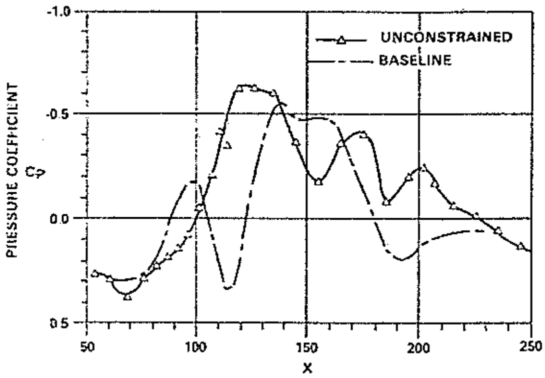

Figure 14 — Comparison of Predicted Pressures on Rotation Unconstrained and Baseline Designs

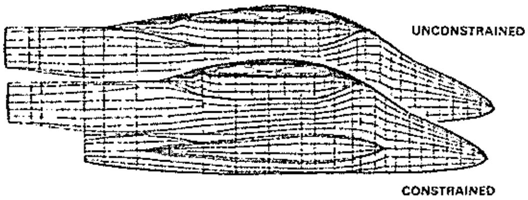

Figure 15 — Comparison of Rotation Constrained and Unconstrained Fairing Designs

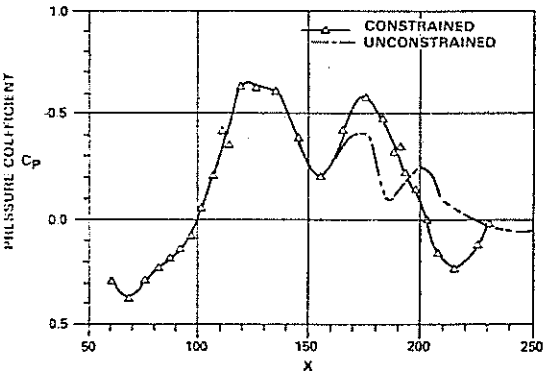

Figure 16 — Comparison of Predicted Centerline Pressures on Constrained and Unconstrained Fairings

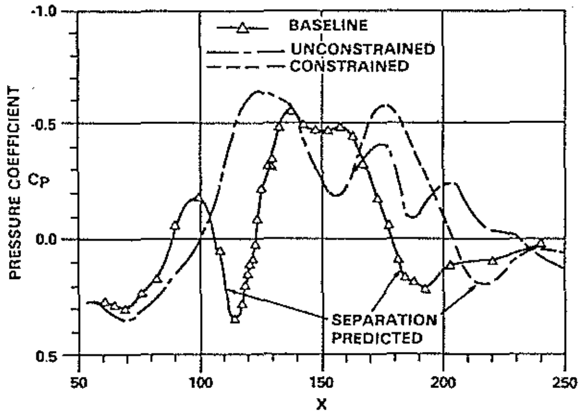

Figure 17 — Effect of Fairing Shape on Predicted Centerline Pressures

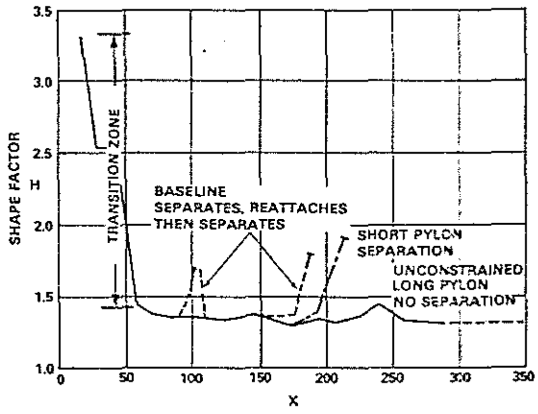

Figure 18 — Effect of Hub-Pylon Shape on Centerline Boundary Layer Characteristics

GPO 860 025